Development 130, 1037-1048

doi:10.1242/dev.00326

Irx4-mediated regulation of *Slit1* expression contributes to the definition of early axonal paths inside the retina

Zhe Jin[1], Jinhua Zhang[1], Avihu Klar[2], Alain Chédotal[3], Yi Rao[4], Constance L. Cepko[5] and Zheng-Zheng Bao[1,*]

[1]Department of Medicine, University of Massachusetts Medical School, 364 Plantation Street, Worcester, MA 01605, USA
[2]Department of Anatomy and Cell Biology, The Hebrew University-Hadassah Medical School, PO Box 12272, Jerusalem 91120, Israel
[3]Institut de la Santé et de le Recherche Médicale U106, Bâtiment de Pédiatrie, Hôpital de la Salpêtrière, 47 Boulevard de l'Hôpital, 75013, Paris, France
[4]Department of Anatomy and Neurobiology, Washington University School of Medicine, Box 8108, 660 S. Euclid Avenue, St Louis, MO 63110, USA
[5]Department of Genetics, Harvard Medical School, 200 Longwood Avenue, Boston, MA 02115, USA
*Author for correspondence (e-mail: zheng.bao@umassmed.edu)

Accepted 6 December 2002

SUMMARY

Although multiple axon guidance cues have been discovered in recent years, little is known about the mechanism by which the spatiotemporal expression patterns of the axon guidance cues are regulated in vertebrates. We report that a homeobox gene *Irx4* is expressed in a pattern similar to that of *Slit1* in the chicken retina. Overexpression of Irx4 led to specific downregulation of *Slit1* expression, whereas inhibition of Irx4 activity by a dominant negative mutant led to induction of *Slit1* expression, indicating that Irx4 is a crucial regulator of *Slit1* expression in the retina. In addition, by examining axonal behavior in the retinas with overexpression of Irx4 and using several in vivo assays to test the effect of Slit1, we found that Slit1 acts positively to guide the retinal axons inside the optic fiber layer (OFL). We further show that the regulation of *Slit1* expression by Irx4 is important for providing intermediate targets for retinal axons during their growth within the retina.

Key words: Irx4, Slit1, Retinal axon, Expression regulation, chick

INTRODUCTION

During development, axons navigate through 3D space in long, specific paths to establish neuronal connections. In visual system development, one of the early events is intra-retinal axon targeting. Extended from the ganglion cells (RGC) in the ganglion cell layer (GCL), the axons travel in a thin optic fiber layer (OFL) at the vitreal surface. Within OFL, all ganglion axons project towards the optic disc at the center of the retina, where they exit the eye (Fig. 1) (Halfter, 1985; Thanos and Mey, 2001). Within the retina, the newly extended immature axons join and leave fascicles, producing a type of 'honeycomb' appearance. The axons soon mature into straight and fasciculated axon bundles.

Several molecules have been reported to be involved in the central projection of retinal axons toward the optic disc. Chondroitin sulfate proteoglycans, a major component of the ECM, are suggested to act as inhibitory molecules to prevent the growth of retinal axons towards the periphery (Brittis et al., 1992). In netrin 1/DCC or the EphB ligand-deficient mouse embryos, RGC axon pathfinding defects have also been observed near the optic disc (Birgbauer et al., 2000; Deiner et al., 1997). L1, receptor tyrosine phosphatase, have also been shown to be involved in axonal outgrowth or projection inside the retina (Brittis et al., 1995; Ledig et al., 1999; Snow et al., 1991). However, the molecular mechanisms involved in guiding the retinal axons specifically within the OFL are not fully understood.

Genetic, biochemical and molecular approaches have led to the identification of an increasing number of molecules as axon guidance cues (reviewed by Brose and Tessier-Lavigne, 2000; Mueller, 1999; Raper, 2000; Yu and Bargmann, 2001). Slit proteins are large secreted glycoproteins of ~200 kDa, comprising four leucine rich repeats, seven to nine EGF repeats and a Laminin G-like module. Three distinct Slit genes, *Slit1*, *Slit2* and *Slit3*, have been cloned in mammals (Brose et al., 1999; Holmes et al., 1998; Itoh et al., 1998; Li et al., 1999). In tissue culture, Slit1 and Slit2 proteins have been shown to function as chemorepellents and collapsing factors for olfactory, motor, hippocampal and retinal axons (Erskine et al., 2000; Li et al., 1999; Nguyen Ba-Charvet et al., 1999; Niclou et al., 2000; Plump et al., 2002; Ringstedt et al., 2000). Slit1 and Slit2 also repel tangentially migrating interneurons in the mouse telencephalon (Hu, 1999; Zhu et al., 1999). However, Slit can also act positively on the axons. Slit2 stimulates the formation of axon collateral branches of the sensory neurons (Wang et al., 1999). In *Drosophila*, migrating mesodermal cells can switch their response to Slit from repulsion to attraction

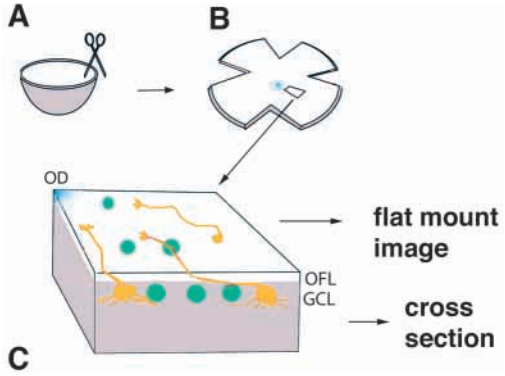

Fig. 1. Intra-retinal axon targeting. (A) To facilitate analysis and observation, retinas were flat-mounted by making a few cuts at the edge. (B) The cells in the GCL and the axons in OFL can be stained and analyzed on the flat-mount retina with the vitreal side upwards. (C) Retinal ganglion cells in ganglion cell layer (GCL) extend axons to optic fiber layer (OFL) where they project towards the optic disc (OD) at the center of the retina.

(Kramer, 2001). Robo proteins have been characterized as the receptors for Slits (Brose et al., 1999; Kidd et al., 1999). In mouse, *Slit1*, *Slit2*, *Robo1* and *Robo2* (from the Slit/Robo family) have been reported to be expressed in the ganglion cell layer (GCL) in the retina (Erskine et al., 2000; Niclou et al., 2000; Ringstedt et al., 2000). Slit1, Slit2 and Robo2 control the midline crossing of the axons at the optic chiasm (Hutson and Chien, 2002; Plump et al., 2002). However, their roles in intra-retinal axon pathfinding remain unclear.

Interestingly, several members of the Irx homeobox gene family, including *Irx4*, are also expressed in GCL in retina (Bruneau et al., 2000; Mummenhoff et al., 2001). Irx genes were identified based on the homology to the *Drosophila Iroquois* locus genes. The Irx genes belong to a family of evolutionarily conserved homeobox genes. There are three Iro genes in *Drosophila*, which form the Iroquois complex (Iro-C) (Gomez-Skarmeta et al., 1996; McNeill et al., 1997). Six Irx genes (*Irx1-Irx6*) have been identified in mouse and human, which are located in two genomic clusters of three genes each (Bosse et al., 2000; Bosse et al., 1997; Bruneau et al., 2000; Christoffels et al., 2000; Cohen et al., 2000; Peters et al., 2000). The Irx genes encode transcriptional controllers that contain a characteristic homeodomain and a sequence motif unique to the family, Iro box. The Irx genes function early in development to specify the identity of diverse territories of the body, such as in the head and mesothorax of *Drosophila*, the neural plate of *Xenopus*, vertebrate neural tube and heart (reviewed by Cavodeassi et al., 2001).

To study the molecular mechanisms of retinal axon guidance, we used the chicken system as an in vivo model system because of its experimental accessibility (Nakamoto, 1996). Using both gain-of-function and loss-of-function approaches, we found that Irx4 specifically regulates *Slit1* expression to restrict it to a subset of cells in the ganglion cell layer. We have further analyzed Slit1 function in intra-retinal axon targeting. Our results suggest that Slit1 may act positively to guide retinal axons within the OFL. Irx4 regulation of *Slit1* is important for the formation of the 'honeycomb' appearance of the immature retinal axons within the retina.

MATERIALS AND METHODS

In situ hybridization

Flat-mount and section in situ hybridization with the digoxigenin-labeled probes were carried out as previously described (Bao et al., 1999). For two-color in situ hybridization, one probe was labeled with fluorescein-12-UTP (Roche), while the other probe was labeled with digoxigenin-11-UTP (Roche) by in vitro transcription. The samples were hybridized with both probes simultaneously. The digoxigenin-labeled probe was detected first using an alkaline phosphatase-coupled anti-digoxigenin antibody and the NBT/BCIP substrate. The subsequent detection of the fluorescein-labeled probe was carried out by using an alkaline phosphatase-coupled anti-fluorescein antibody and developed with the Vector Red kit (Vector Laboratories).

Retroviral injection and electroporation

RCAS-Irx4 and RCAS-DN-Irx4 viruses were prepared as previously described (Bao et al., 1999). Viral stocks at 5×10^8 titer were injected into both optic vesicles at Hamburger-Hamilton (HH) stage10-11 (~E1.5) (Hamburger and Hamilton, 1992). Electroporation was also carried out on HH stage 10-11 chick embryos by using a square wave electroporator CUY-21 (Nepa Gene Company). DNA (0.7-1.3 mg/ml) mixed with the Fast Green dye (0.025%) was injected into the right optic vesicle. The positive electrode was placed next to the outer side of the right optic vesicle while the negative electrode was placed onto the forebrain/midbrain region of the embryo. Three pulses of 50 mseconds duration each at 15 V were applied.

Immunofluorescent staining

Immunofluorescent staining was carried out on flat mounts of retina. Axons were stained with either monoclonal antibody 270.7 (provided by Dr Virginia Lee, University of Pennsylvania Medical School) or monoclonal antibody 3A10 in the 'gene-axon assay'. Retinas were fixed in 4% paraformaldehyde, flat mounted and blocked in 10% calf serum DME with 0.2% Triton X-100. Primary and secondary antibodies were diluted in the block and incubated with the samples for 4 hours at room temperature or at 4°C overnight. Viral infection was confirmed by immunofluorescent staining with either the monoclonal antibody 3C2 (diluted 1:5) or the polyclonal antibody p27 (SPAFAS, Norwich, CT; diluted 1:10,000). Mouse monoclonal antibodies against Islet1 (39.4D5), neurofilament (3A10) and Myc (9E10) were purchased from the Developmental Studies Hybridoma Bank (University of Iowa, Iowa City, IA).

For analysis of the electroporated samples, the retinas were harvested at E7 or E7.5, and fixed in 4% paraformaldehyde. The Slit1-electroporated samples were co-immunostained with an anti-neurofilament antibody 270.7 and a rabbit polyclonal anti-Myc antibody followed by Cy3-conjugated donkey anti-mouse and FITC-conjugated donkey anti-rabbit secondary antibodies (Jackson ImmunoResearch Laboratories, West Grove, PN). Rabbit polyclonal anti-Myc antibody was obtained from Immunology Consultants Laboratory (Sherwood, OR) and used at 1:500 dilutions. The control GFP-electroporated samples were stained with antibody 270.7 followed by Cy3-conjugated anti-mouse secondary antibody. Images of anti-Myc and anti-neurofilament staining were taken from the same field and overlaid using Photoshop 6.0 software. To quantify the results, we used mouse anti-Myc antibody (9E10) instead of rabbit anti-Myc antibody for co-staining with the neurofilament. We could thus examine the transfected cells and axons within the same fluorescent channel. To score the percentage of the transfected cells that superimpose with the axon bundles, we selected transfected cells that were approximately in the same focal plane as the axons when viewed from the flat-mounts, and only in areas that had less than 50% axon coverage. Cells that appeared too out of focus were not included because they might be too deep to influence axon pathfinding.

RESULTS

Irx4 specifically regulates the expression of *Slit1* in the retina

Using in situ hybridization experiments on cryosections or flat-mounts of retina, we found that the chicken *Irx4* gene is expressed in a subset of cells in GCL throughout retinal development (Fig. 2A,B), similar to the patterns reported in mouse retina (Bruneau et al., 2000; Mummenhoff et al., 2001). In addition, the *Irx4*-expressing cells appeared to be distributed evenly in GCL across the retina, not concentrated in particular sections of the retina (data not shown). Because a number of Slit/Robo family genes have also been reported to be expressed in GCL in mouse (Erskine et al., 2000; Niclou et al., 2000; Ringstedt et al., 2000), we examined whether similar patterns could be observed in the chicken retina. We found that *Slit1* is expressed in a subset of cells in GCL, not in any other layers, at E4.5, E6 and E9 (Fig. 2C,D, data not shown). Similarly, *Robo1* is also expressed in a subset of the cells in GCL (Fig. 2E). To compare the expression of *Irx4* and *Slit1* in GCL further, we performed two-color in situ hybridization experiments. As shown in Fig. 2F, while some cells express neither gene and a small number of cells appear to have both colors, the majority of the GCL cells express only one of the two genes, either *Irx4* or *Slit1*.

In vertebrates, the underlying mechanism by which the expression of the Slit/Robo family genes is regulated has not yet been reported. Our observation of similar expression patterns of *Irx4* and Slit/Robo family genes in GCL gave us a basis to test whether there is a regulatory relationship between *Irx4* and the Slit/Robo genes. We used a retroviral vector (RCAS) to express the full-length Irx4 protein, RCAS-Irx4 (Fig. 3A) (Bao et al., 1999). This viral construct can produce replication-competent viral particles that infect proliferating cells and express Irx4 protein in the infected cells. Both optic vesicles were injected at Hamburger-Hamilton (HH) stage 10-11 (~E1.5) (Hamburger and Hamilton, 1992) with the viral stocks at appropriate titers to achieve incomplete infection (Schulte and Cepko, 2000). The incomplete infection would result in patches of cells infected surrounded by uninfected area, allowing direct comparison of the area with overexpression of Irx4 with the wild-type area. The infected retinas were harvested at embryonic day 8 (E8) and flat-mounted for the ease of analysis and observation (Fig. 1). After in situ hybridization with various RNA probes or immunofluorescent staining by cell type-specific antibodies, the samples were also immunostained with an antibody specific for viral antigen GAG to show the infected area. By comparing gene expression in the infected area immediately adjacent to the uninfected wild-type area, we were able to assess whether any of the genes was subject to the regulation by Irx4.

In the uninfected area, as in the wild-type control, a subset of GCL cells expressed *Slit1* at a high level, scattered among cells that did not express *Slit1* (Fig. 3B). However, the number of cells expressing *Slit1* was significantly reduced in the area infected with RCAS-Irx4 virus (Fig. 3B,C). In the areas that had relatively large patches of infection, very few cells expressed *Slit1*. The control virus RCAS-GFP expressing a GFP protein did not change the expression of the *Slit1* gene (data not shown), indicating that change of *Slit1* expression was not merely due to viral infection. To examine whether Irx4 overexpression affected ganglion cell specification or differentiation, we analyzed all the GCL-specific markers available to us, including *Brn3a*, *Brn3b* (Liu et al., 2000), RA4 (McLoon and Barnes, 1989), nicotinic acetylcholine receptor β 3 (Hernandez et al., 1995), and islet 1 (Austin et al., 1995). The expression of these markers was not altered in the samples infected with the RCAS-Irx4 virus (data not shown, Fig. 3F,G). Within the Slit/Robo family genes, the expression of *Slit2*, *Robo1* and *Robo2* was also unaffected by Irx4 overexpression (Fig. 3D,E, data not shown). These results demonstrate that Irx4 specifically downregulates the expression of *Slit1* in GCL.

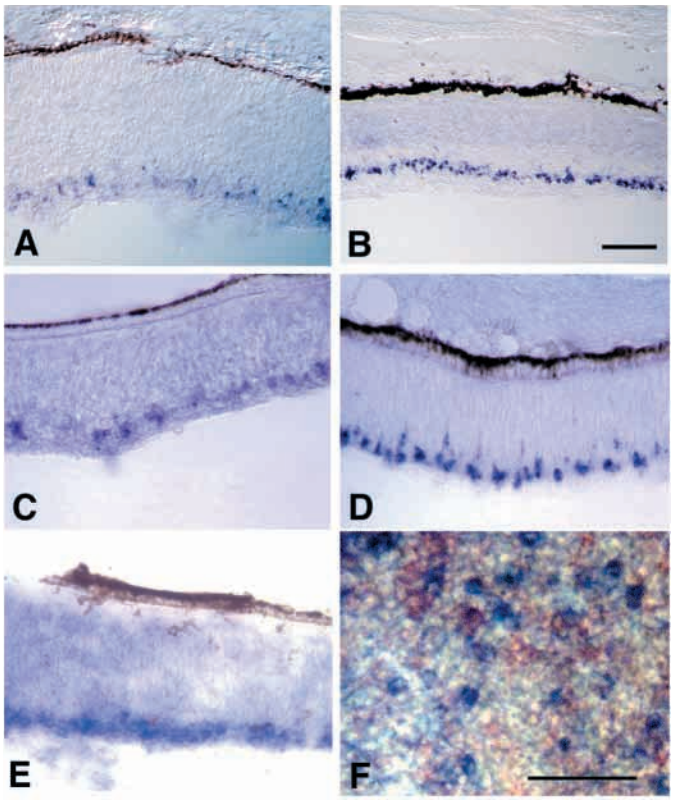

Fig. 2. mRNA expression of *Irx4* and the *Slit/Robo* family genes in chicken retina. In situ hybridization with various probes on retinal sections: (A) *Irx4* probe, E7 retina; (B) *Irx4* probe, E12 retina; (C) *Slit1* probe, E4.5 retina; (D) *Slit1* probe, E6 retina; (E) *Robo1* probe, E9 retina. Note that *Irx4*, *Slit1* and *Robo1* are all expressed in subsets of cells in GCL. (F) Two-color in situ hybridization on E7 flat-mount retina, with *Slit1* (fluorescein-labeled, shown as red) and *Irx4* probes (DIG-labeled, shown as purple). Note that *Slit1* and *Irx4* are mostly localized in two distinct cell populations in GCL. Scale bars: 100 μm.

Irx4 function is required for the repression of *Slit1* expression

We next examined whether Irx4 function is required for the repression of *Slit1* expression in the retina. We used a dominant-negative Irx4 construct, RCAS-DN-Irx4, which encodes a fusion protein composed of the chicken Irx4 homeodomain and the repressor domain of the *Drosophila* Engrailed protein (Fig. 3A) (Bao et al., 1999). Fusion of a DNA-binding domain, such as a homeodomain with the repressor domain of Engrailed, can create a protein that

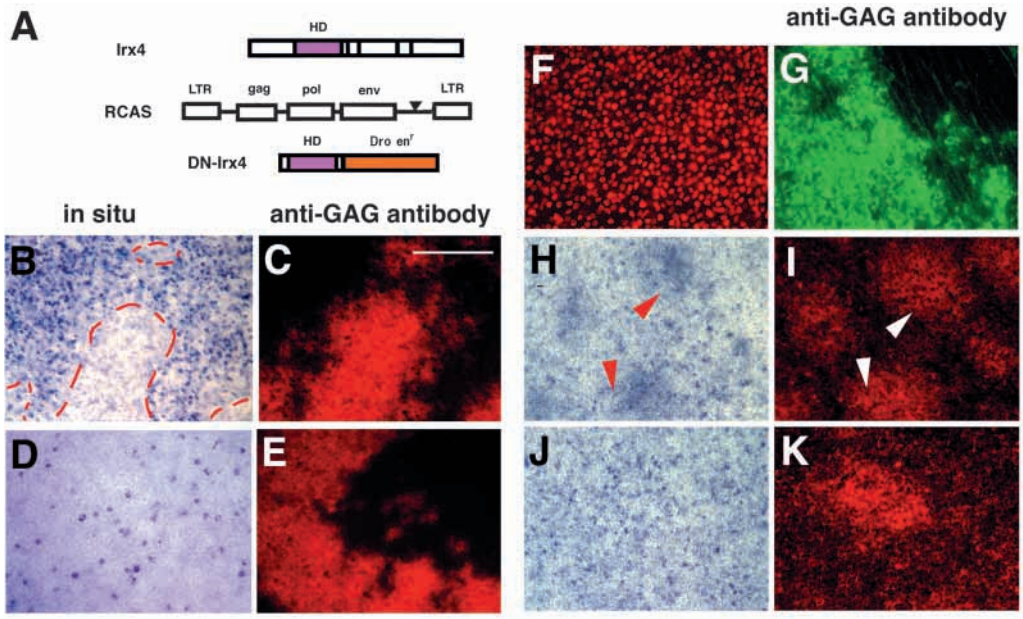

Fig. 3. Irx4 specifically downregulates the expression of *Slit1* in GCL. (A) Replication-competent retroviral constructs for expressing full-length Irx4 protein (RCAS-Irx4) or dominant-negative Irx4 protein (RCAS-DN-Irx4). (B-G) Retinas infected with the RCAS-Irx4 virus were hybridized with the Slit1 probe (B) or Robo1 probe (D), or stained with anti-Islet 1 antibody (F). All samples were also stained with the anti-viral GAG antibody to show the area of infection (C,E,G). Note the RCAS-Irx4-infected areas had few *Slit1*-expressing cells (marked with red broken lines). The samples infected with the dominant-negative Irx4 virus (H,I) or the control virus expressing only the Engrailed repressor domain (J,K) were similarly hybridized with the Slit1 probe (H,J) and stained with the anti-viral GAG antibody (I,K). Note the *Slit1* expression was activated in the areas infected with the RCAS-DN-Irx4 virus (arrowheads in H,I) but not the control virus. Scale bar: 100 μm.

interferes with transcriptional activation by the wild-type protein (Badiani et al., 1994). The retinas were similarly infected by RCAS-DN-Irx4 and analyzed by in situ hybridization at E8. Although *Slit1* was expressed in a subset of cells in the uninfected area, the infected area appeared to have substantial upregulation of *Slit1* expression. The infected area appeared as round patches within which most if not all cells are expressing *Slit1* (Fig. 3H,I). Dominant-negative Irx4 did not have any effect on the expression of *Slit2*, *Robo1* or *Robo2* (data not shown). Control virus encoding only the Engrailed repressor domain did not have any effect on *Slit1* expression (Fig. 3J,K). This indicates that disruption of Irx4 function can relieve the repression of *Slit1* expression in the cells.

The negative regulatory relationship between *Irx4* and *Slit1* is consistent with the two-color in situ hybridization result that *Irx4* and *Slit1* are mostly expressed in distinct cell populations in GCL (Fig. 2F). Although a small number of cells appear to have both colors, it is difficult to determine whether these cells express both genes, or the enzyme detecting the first probe was not completely inactivated. Two-color in situ hybridization is technically difficult especially at the resolution of single-cell level. Recently, we found that *Slit1* expression decreases from E7 (data not shown). It is possible that *Irx4* may be involved in downregulation of the expression of *Slit1* after the axons have reached the optic disc. The overlapping expression in a small number of cells may be due to upregulation of *Irx4* and downregulation of *Slit1* expression at later stages.

Overexpression of Irx4 interferes with intra-retinal axon targeting

Although *Slit1* is known to function in axon pathfinding (Brose et al., 1999; Kidd et al., 1999; Li et al., 1999; Nguyen Ba-Charvet et al., 1999; Wang et al., 1999), its role in intra-retinal axon guidance has not been reported. We analyzed the intra-retinal axon pathfinding in the samples with reduced *Slit1* expression by infection with the RCAS-Irx4 virus. Infected with the RCAS-Irx4 virus or a control RCAS-GFP virus at HH stage 10-11 (E1.5) before the onset of ganglion cell differentiation at E4, the retinas were analyzed at E7, E8 or E12 on flat-mounts. Because retinal axons travel in the OFL, flat-mounts of retina allowed us to examine readily the trajectory of the axons from the vitreal side. Axons were immunostained with an anti-neurofilament antibody (270.7, red) and viral infection was stained using an anti-viral GAG antibody (P27, green).

E7 and E8 were chosen because different stages of axon projection and maturation could be viewed within one retina. There is a center-to-periphery gradient in terms of progression of cell differentiation and axon maturation, the center of the retina being relatively more advanced. As shown in Fig. 4A, axons at the periphery of the E8 retina are relatively immature. They join and leave fascicles, producing a type of honeycomb appearance. At the median to center of the retina, however, the axons are more mature, more fasciculated and relatively straight (Fig. 4B). At E7, larger area of the peripheral retina appears immature, whereas at E12, axons in the entire retina appear fasciculated and straight.

In the control virus RCAS-GFP-infected retinas, the axons appeared completely normal in the infected area, suggesting that viral infection alone did not affect intra-retinal axon pathfinding (Fig. 4C,D). However, in the RCAS-Irx4 virus-injected retinas, the axons appeared to distribute unevenly and were overly fasciculated, although the axons still projected towards the optic disc (Fig. 4E-H; Fig. 5). Upon closer inspection, the areas with axonal abnormality were all within the regions that were infected with the RCAS-Irx4 virus. Close to the border of the infected/uninfected area, the axons appeared to avoid the infected area and turned in order to be in the uninfected area (Fig. 4E,F; Fig. 5A-D). This resulted in

uneven distribution of the axons, such that the wild-type area had more and denser axon bundles than did the infected area. Because the infected area had a much lower level of *Slit1* expression compared with the wild type area (Fig. 3B,C), the preference of the axons for the normal level of *Slit1* in the wild-type area suggests that Slit1 is likely to act positively on the axons.

Although the axons at the infected/uninfected border appeared to turn to avoid the infected areas, the axons in the center of the infected area did not turn visibly (Fig. 4E-H; Fig. 5A-D), suggesting that the axons do not respond to Slit1 from a long range. However, many of the axons in the middle of the infected area appeared excessively fasciculated. This is especially evident when the axons projected perpendicularly through a uninfected/infected boundary (Fig. 4G,H). When the axons went from the uninfected area (UI) to an infected area (Ib), the overall direction of axon projection towards the optic disc was not affected. However, an increase in fasciculation occurred at the boundary, which caused an abrupt decrease of the number of axon bundles in the infected area. Because fasciculation is generally believed to be a response to repellents, the uninfected area with normal amount of Slit1 appeared more attractive or permissive, while the infected area with low amount of Slit1 was more repulsive or unpermissive to the axons. However, excessive fasciculation in infected area was also reversible. As the axons went from an infected area (Ia) to an uninfected area (UI), they returned to the appearance of the control with a significant increase in number of axon bundles, presumably by defasciculation (Fig. 4G,H). This suggests that the axonal abnormality is a response to the environment, not a permanent change within the axons.

There is a positive correlation between the infection and axonal abnormality. Most of the RCAS-Irx4-infected patches exhibited axonal phenotypes described above: avoidance of the infected area and excessive fasciculation. We excluded very small infected patches that contained less than 50 cells because we felt that the newly infected patches might not have enough time to downregulate *Slit1* and cause a phenotype (indicated by an asterisk * in Fig. 5A-D). Of a total of 177 RCAS-Irx4-infected patches (from 38 retinas) from four independent experiments, 162 of them (91.2%) have the avoidance and fasciculation axonal phenotypes. By contrast, we never observed any axonal phenotype in control RCAS-GFP-infected retinas (0%, n=43 patches). In addition, the axons appeared to respond to the *Slit1*-low area only when they were passing through it. Once they had passed, they did not move out of the way as the area became Slit1-negative. At later stages (such as E12), the retinas were usually completely infected (data not shown). But the affected areas were still restricted, comparable with earlier stages (Fig. 5E). These results demonstrate that overexpression of Irx4 leads to abnormal retinal axon trajectories inside the retina.

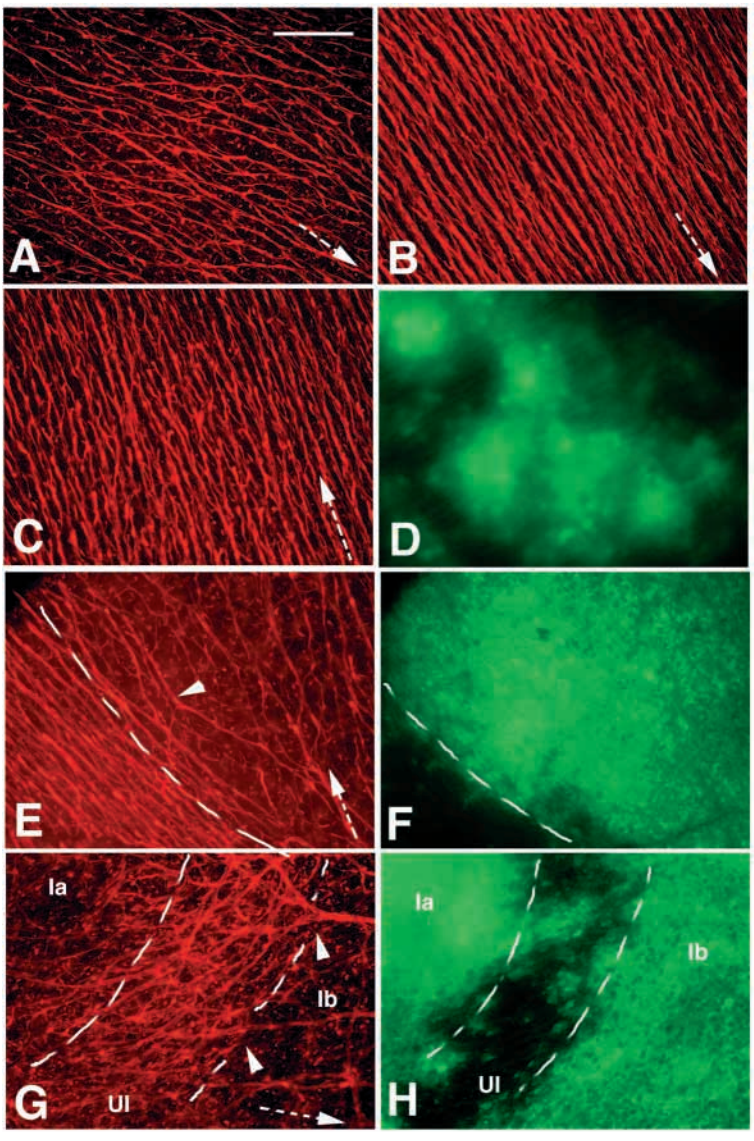

Fig. 4. Intraretinal axonal phenotype caused by RCAS-Irx4 virus infection. Retina development is more advanced in the center than in the periphery. The axons in the wild-type E8 retina were stained with the anti-neurofilament antibody 270.7 (A,B). (A) At the periphery, axons join and leave fascicles, producing a 'honeycomb' appearance. (B) Close to the center of the retina, the axons appear more mature and fasciculated. (C-H) Optic vesicles were infected with RCAS-Irx4 virus (E-H) or control RCAS-GFP (C,D) at HH stage 10-11 (E1.5) and the infected retinas were harvested at E8. Flat-mounts of retinas were double stained with a mouse monoclonal antibody recognizing neurofilament (270.7) (C,E,G) and a rabbit polyclonal antibody recognizing viral antigen (anti-p27) (D,F,H). Images in C,E and G are in the same fields as in D,F and H, respectively. The broken white arrows in A-C,E,G indicate the direction of axon projection toward the optic disc. (C,D) The axons in the control RCAS-GFP virus-injected retina appear normal. (E,F) Close to the infected/uninfected boundaries, some axons appear to turn slightly towards the uninfected area (arrowhead in E). (G,H) In the center of the infected area, an abrupt increase of fasciculation of the axon bundles was observed (arrowheads in G) when axons went from an uninfected (UI) to an infected (Ib) area. The axons returned to wild-type appearance when they went from infected (Ia) to uninfected (UI) area, suggesting that the changes in axonal morphology in the infected area were reversible. Scale bar: 100 μm.

Slit1 acts positively on the retinal axons inside the retina

As vertebrate Slits have been reported mostly as repellents in other assay systems (Erskine et al., 2000; Li et al., 1999; Niclou et al., 2000; Plump et al., 2002; Ringstedt et al., 2000) and our results with Irx4 overexpression suggest that Slit1 may act positively on the retinal axons within the retina, we set out to develop an in vivo assay for testing the effect of Slit1 inside the retina. Because *Slit1* is too large to be expressed by a retroviral vector, we used electroporation to deliver an expression construct of Slit1 into the optic vesicles. Unlike retroviral infection, the transfected cells appeared as a group of scattered individual cells (Fig. 6D-G).

The rational behind the in vivo assay is described below. As shown in Fig. 6A, the axons travel in the very thin optic fiber layer (OFL) above GCL. At E7, there are only two cellular layers in the retina: GCL and the deeper layer containing mainly undifferentiated cells. In flat-mounts, we were able to score the relative positions of the transfected cells in GCL with the axons in OFL. Other transfected cells located deeper would not be in the same focal plane as the axons when viewed from the vitreal side of the flat-mounts. Because they might be too far away to have any influence on the axons, we did not score these cells. If the protein acts positively, the axons would prefer to grow on top of the transfected cells in GCL, superimposed on the transfected cells (Fig. 6B). Conversely, if the protein acts negatively, the axons would avoid the transfected cells, thus would not be superimposed on the transfected cells (Fig. 6C). If the protein has no effect on the axons, such as a GFP protein, the axons would appear to distribute randomly relative to the positions of the transfected cells.

As a control, we electroporated an expression construct encoding GFP into the optic vesicles at HH stage 10-11. The retinas were harvested at E7 and the axons were stained with an anti-neurofilament antibody (270.7) followed by Cy3-conjugated anti-mouse secondary antibody. Some GFP-expressing cells were clearly visible from the vitreal side of the flat-mount retinas, approximately in the same focal plane of the axons, indicating they were the transfected cells in GCL (Fig. 6E,G). Other cells that were localized deeper and difficult to be seen in the focal plane of the axons were not scored. We also scored only in the area with less than 50% of axon coverage (median to periphery of the retina), because the axons were very dense at the vicinity of optic disc. In these control samples, the localization of the control GFP-transfected cells appeared random relative to the axon bundles (Fig. 6E,G). Forty-six percent of the control GFP-transfected cells (n=398, from 12 retinas) have axons growing on top of them.

To test the function of Slit1, we electroporated an expression construct encoding a Myc-tagged Slit1 (pCS2-Slit1myc) (Wu et al., 1999) into the optic vesicles at HH stage 10-11. The retinas were analyzed at E7. The *Slit1*-transfected cells were identified by a rabbit anti-Myc antibody, while the axons were stained with a mouse anti-neurofilament antibody, 270.7 (Fig. 6D,F). Interestingly, most of the *Slit1*-transfected cells appeared to have axons passing on top of them (magenta circles, Fig. 6D,F). To quantify the data, we used a mouse anti-Myc antibody (9E10) to co-stain with the mouse anti-neurofilament antibody (270.7) so that we were able to compare the relative positions within one fluorescence channel. A total of 563 cells from 24 retinas were scored in the area that had less than 50% of axon coverage in three independent experiments. Slit1-transfected cells (91.1%) have axon bundles growing over them. Compared with the control GFP-transfected cells, the axons appeared to travel preferentially above the *Slit1*-expressing cells. These results suggest that Slit1 may act positively on the growth of the retinal axons.

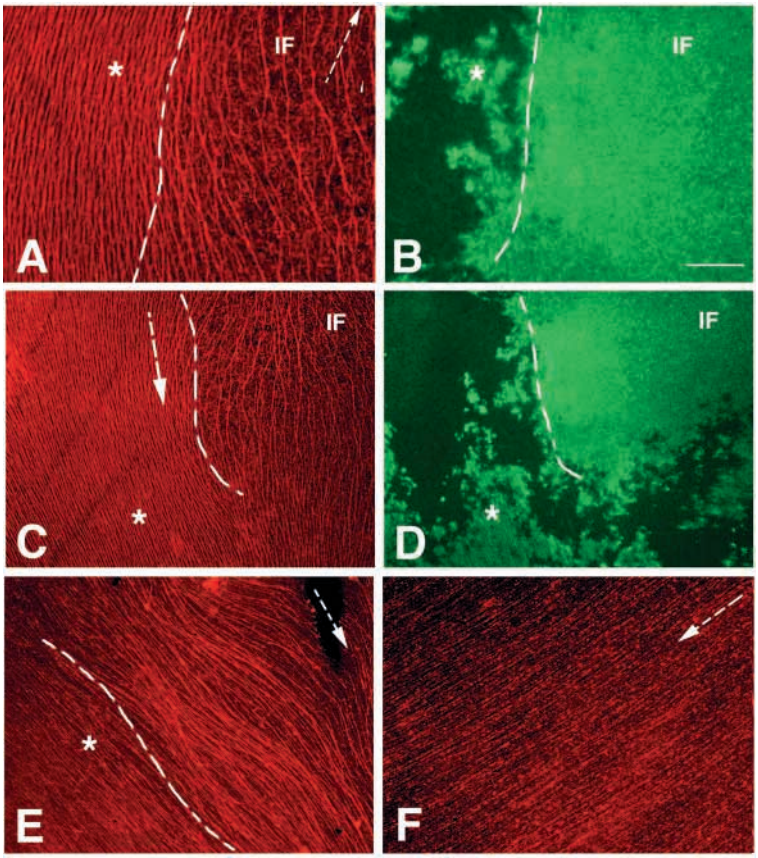

Fig. 5. Intraretinal axonal phenotype caused by RCAS-Irx4 virus infection, viewed at lower magnification. The retinas were infected at stage 10-11 and harvested at E7 (A-D) or E12 (E,F). Axons were stained with an anti-neurofilament antibody (A,C,E,F), whereas the infected area was visualized by staining with an anti-viral GAG antibody (p27) (B,D). Images in A,C are in the same fields as in B,D, respectively. The broken white arrows in A,C,E,F indicate the direction of axon projection towards the optic disc. Note the axons turned to avoid the infected area (marked with IF in A,C). However, the area that exhibited phenotype was smaller than the infected area. Some newly infected areas with only scattered infection (marked with and asterisk in A-D) did not show axonal abnormality. (E) At E12, the retina was completely infected with the RCAS-Irx4 virus (data not shown); however, the area with the phenotype did not expand to the entire retina. Some areas still appeared normal (marked with an asterisk), indicating that axons no longer responded to low Slit1 levels after they had passed through the area. (F) The axons in the control virus RCAS-GFP-infected retina appeared completely normal at E12. Scale bar: 200 μm.

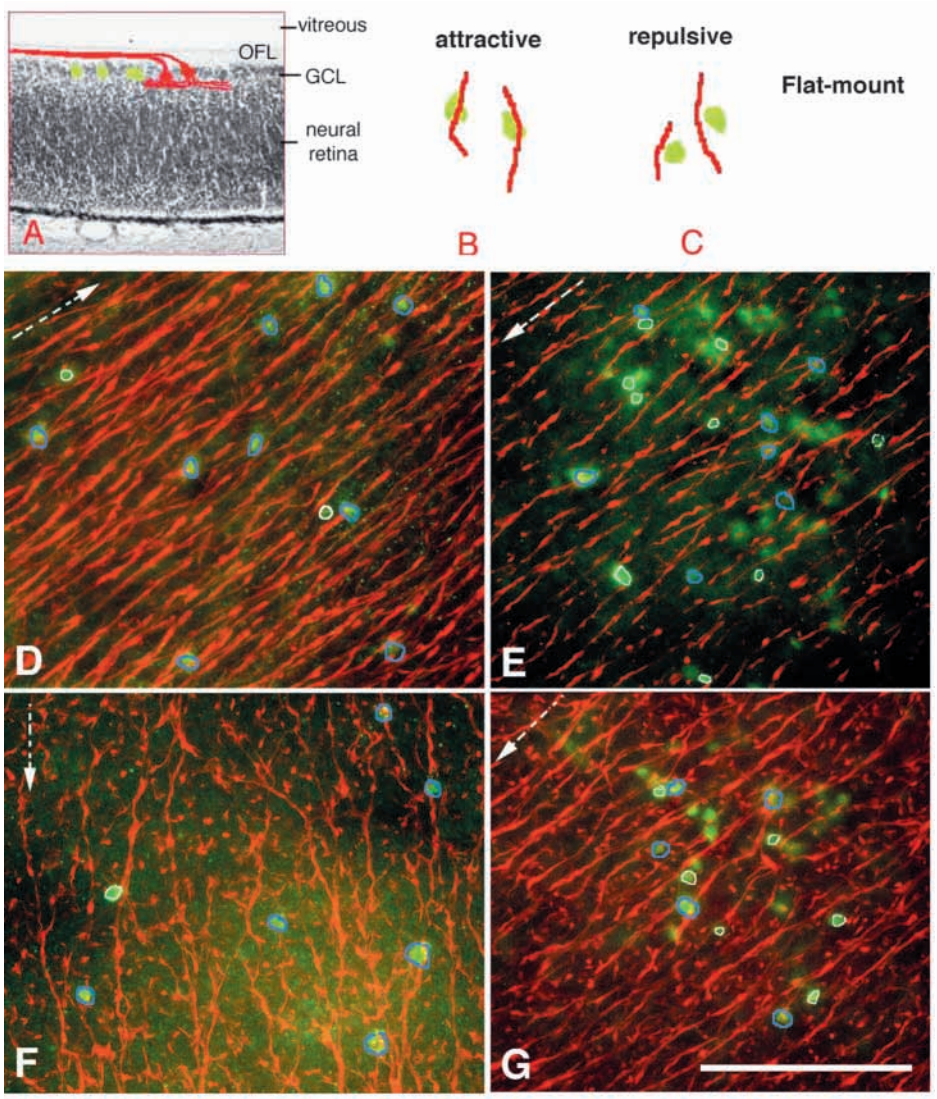

Fig. 6. In vivo assay to test the function of Slit1 in retina. (A-C) Design of the in vivo assay. (A) A full-length Myc-tagged Slit1 expression construct was transfected into retinal cells by in ovo electroporation. The transfected cells were identified using anti-Myc antibody (green), whereas the axons were stained with anti-neurofilament antibody (red). Because some transfected cells will be localized in the cellular GCL, immediately beneath OFL where the retinal axons travel, we will be able to determine the effect of Slit1 on axons by comparing the relative positions of the *Slit1*-transfected cells and the axons. (B) If Slit1 is attractive to axons, axons will preferentially overlie the Slit1-transfected cells, appearing superimposed on the cells. (C) Alternatively, if Slit1 is repulsive to axons, the axons will avoid the transfected cells, thus not becoming superimposed on the cells. The actual data of Slit1 transfection are shown in D and F. Most of the Slit1-transfected cells align with the axon bundles (blue circles). (E,G) The control GFP-transfected cells, however, appear random with regard to the position of the axons. The blue circles indicate the cells that align accurately with the axons while the white circles indicate the cells that do not align with the axons. The broken white arrows in D-G indicate the direction of axon projection towards the optic disc. Scale bar: 150 μm.

The axonal phenotype of Irx4 overexpression can be rescued by Slit1

To confirm that the axonal phenotype of Irx4 overexpression is due to decreased *Slit1* expression, and not other molecule(s) regulated by Irx4, we tested whether Slit1 could rescue the phenotype. We co-electroporated RCAS-Irx4 construct with the Slit1 expression construct in ovo at HH stage 10-11. The retinas were analyzed at E8 by co-staining with anti-Myc (9E10, red), anti-GAG (P27, green) and anti-neurofilament (270.7, red) antibodies to show the Slit1-transfected cells, RCAS-Irx4-infected cells and axons, respectively. RCAS-Irx4 virus was made in the cells transfected with the RCAS-Irx4 construct, and rapidly spread inside the retina. However, the expression construct of Slit1 could not produce virus and Slit1 would only be expressed in the cells that were transfected. Therefore, the RCAS-Irx4-infected area was much larger than the area containing the *Slit1*-transfected cells. Slit1-transfected cells appeared as patches of scattered cells expressing Myc-tag (Fig. 7A-C).

In the area that had both RCAS-Irx4 infection and a large number of *Slit1*-transfected cells, the axons appeared largely normal, evenly distributed and dense (Fig. 7A,B). However, in the area with RCAS-Irx4 infection but no *Slit1*-transfected cells, the axons were excessively fasciculated and unevenly distributed (marked with NR in Fig. 7B), similar to the axons in the control experiments in which a GFP expression construct was co-electroporated with the RCAS-Irx4 construct (Fig. 7E). When only a small number of Slit1-transfected cells were present, the axonal phenotype was not fully corrected but did appear improved (Fig. 7C). Interestingly, most of the transfected cells had axons passing on top of them (Fig. 7C). From three independent experiments, 100% of the retinas (n=23) that were co-electroporated with the Slit1 expression construct showed improvement in axonal appearance: axons were more even and not as excessively fasciculated as in the retinas injected with the RCAS-Irx4 virus alone. No improvement in axonal phenotype was observed in the samples that were co-electroporated with the GFP construct (0%, n=11). These results demonstrate that Slit1 can rescue the axonal phenotypes caused by Irx4 overexpression.

Slit1 contributes to the definition of early axonal paths inside the retina

To determine how the endogenous Slit1 influences the retinal

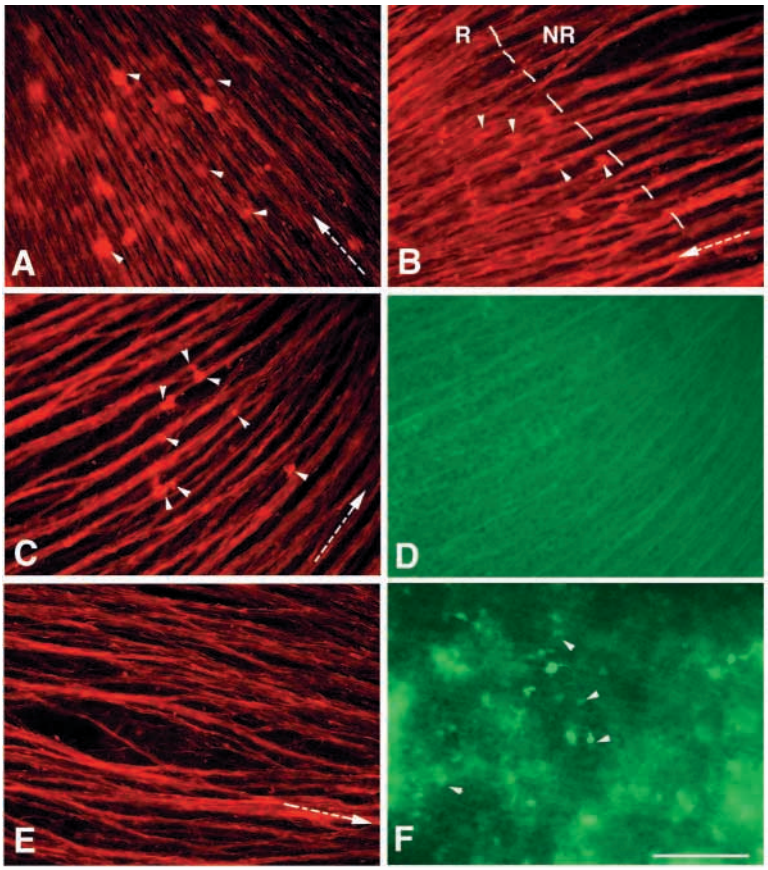

Fig. 7. Slit1 can rescue the axonal phenotype caused by RCAS-Irx4 infection. Slit1 expression construct was co-electroporated with the RCAS-Irx4 construct. As the RCAS-Irx4-transfected cells would produce infectious viral particles that spread inside the retina, the infected area was larger than the *Slit1*-transfected area. Note in the area where a large number of *Slit1*-transfected cells were present (R in B; arrowheads in A,B), axonal phenotypes caused by RCAS-Irx4 infection were largely corrected. However, in the area that did not have *Slit1*-transfected cells (marked with NR in B), the axons were unevenly distributed and excessively fasciculated. (C) In the area where only a small number of Slit1-transfected cells were present, axonal phenotype was partially corrected. Interestingly, most of the transfected cells appear to align accurately with the axon bundles (arrowheads in C). The area shown in A-C was completely infected by RCAS-Irx4, confirmed by anti-GAG staining (D and data not shown). (E,F) As a control, an expression construct encoding GFP was co-electroporated with the RCAS-Irx4 construct. Although a large number of GFP-transfected cells were present in this area (visible over the staining of anti-GAG antibody, arrowheads in F), GFP could not rescue the axonal phenotype of RCAS-Irx4 infection and the axons appeared uneven and excessively fasciculated (E). The broken white arrows in A-C,E indicate the direction of axon projection toward the optic disc. Scale bar: 100 μm.

axon trajectory, we developed another assay (‘gene-axon assay’) to visualize endogenous *Slit1* gene expression simultaneously with axon trajectory. In situ hybridization was carried out on flat-mount retinas with the *Slit1* probe, followed by immunofluorescent staining of axons by an anti-neurofilament antibody 3A10. 3A10 was selected because it was able to recognize the denatured neurofilament antigen after in situ hybridization procedure.

Under a fluorescent microscope, we were able to observe the axons that were fluorescently labeled as well as the dark in situ hybridization signals of the *Slit1* gene (Fig. 8A-E). The staining of 3A10 appeared somewhat fragmented, possibly because the neurofilament antigen was partially digested by treatment of proteinase K during in situ hybridization procedures. As shown in Fig. 8A-D, most of the growth cones of the elongating axons pointed directly toward the cells expressing *Slit1* (arrowheads) and the axons traveled on top of the *Slit1*-expressing cells (Fig. 8A,B). These results support our electroporation data that the endogenous Slit1 appears to act positively on the retinal axons. Because several axons converge on one *Slit1*-positive cell, and then leave separately to go to the next *Slit1*-positive cells (Fig. 8A,B), the interaction of the growth cones and Slit1 appears to contribute to the production of the honeycomb appearance of the early retinal axons (see model, Fig. 8F). These results suggest that Slit1 provides intermediate targets for the retinal axons to travel through the optic fiber layer.

However, as the axons mature into relatively straight thick bundles, similar to those close to the center of the retina, they no longer align accurately with the *Slit1*-expressing cells (Fig. 8E). Some other factors may over-ride the influence of Slit1 by this stage. In addition, the gene-axon assay is also useful for distinguishing the cell type that is expressing *Slit1* in GCL. Because of a lack of suitable molecular markers for the two types of cells in GCL: ganglion cells and displaced amacrine cells, it remains unclear which cell type is expressing *Slit1*. From the result of the gene-axon assay, the axons appear to extend from the cells that are not expressing *Slit1* (marked with a ‘?’ in Fig. 8D), and *Slit1*-expressing cells do not have axons (marked with an asterisk in Fig. 8C,D). This result suggests that *Slit1* is likely to be expressed in the cells without axons, i.e. the displaced amacrine cells, but not in the ganglion cells.

DISCUSSION

In summary, we have shown that Slit1 plays an important role in intra-retinal axon targeting by providing intermediate targets to the retinal axons in OFL. We further demonstrate that *Slit1* expression in GCL is regulated by a homeodomain protein, Irx4. Because multiple guidance cues and many axons are present in vivo, precise spatiotemporal regulation of these guidance cues and receptors ensures correct axon pathfinding in three-dimensional space. In *Drosophila*, it has been reported that transcription factors including Single-minded, Fish-hook, Drifter and Lola are involved in regulating the expression of the *Slit* gene in the midline (Crowner et al., 2002; Ma et al., 2000). However, in vertebrates, the mechanisms by which the

expression of the Slit/Robo family genes is regulated have not yet been reported. We have shown that Irx4 participates in regulation of *Slit1* expression in the retina by using both gain-of-function and loss-of-function approaches. However, our two-color hybridization results also indicate that additional proteins may be involved in repression of *Slit1* expression in GCL, because there are cells that express neither *Irx4* or *Slit1*. We now have evidence that other Irx proteins are involved in regulation of *Slit1* gene expression in GCL (Z. J. and Z.-Z. B., unpublished). Therefore, the dominant-negative Irx4 construct probably acts as dominant-negative for other Irx proteins as well. Further study is required to understand the significance of the involvement of multiple Irx genes in regulation of *Slit1* expression.

Irx genes have been shown to function to subdivide territories into smaller domains. In our study, we have shown that Irx4 regulates gene expression in a subset of cells in the GCL instead of specifying domains. In the samples infected with either the RCAS-Irx4 or RCAS-DN-Irx4, no obvious changes in retinal cell differentiation have been detected. As the Engrailed repressor fusion construct acted as a dominant-negative of the full length Irx4, Irx4 is most probably a transcription activator. Regulation of *Slit1* expression by Irx4 is therefore indirect, mediated through another transcription repressor. It is also interesting to note that the area with decreased *Slit1* expression by Irx4 overexpression matched well with the area of viral infection, indicating a relatively rapid response to Irx4 overexpression.

Most guidance cues are now known to be bi-functional: they can act positively as attractants for one navigational event and negatively as repellents for another (Mueller, 1999; Song and Poo, 1999; Tessier-Lavigne and Goodman, 1996). Recent findings indicate that this bi-functionality can be attributed to differential receptor activation (Hong et al., 1999) or different levels of second messengers in the neuronal cytoplasm, such as the levels of cytoplasmic cAMP/cGMP (Song and Poo, 2001). Many extracellular ligands, including neuromodulators, adhesion molecules and ECM components, can change the level of cyclic nucleotides and are thus capable of modulating axon navigation when they are present concurrently with the guidance cue (Hopker et al., 1999; Nguyen-Ba-Charvet et al., 2001). Interestingly, the same guidance cue can also serve as attractant and repellent for different parts (dendrite versus axon) of the same neuron (Polleux et al., 2000). Thus, the bi-functionality of guidance molecules reflects more the status of the neuron than an intrinsic property of the molecule.

Like most of the guidance cues, Slit can act as a repellent or as an attractant, although mostly as a repellent (Brose et al., 1999; Hu, 1999; Kidd et al., 1999; Kramer, 2001; Li et al., 1999; Nguyen Ba-Charvet et al., 1999; Wang et al., 1999; Wu et al., 1999; Yuan et al., 1999). It can also act both as a short-range and a long-range cue (Kidd et al., 1999; Rajagopalan et al., 2000; Simpson et al., 2000). Several lines of evidence in our study suggest that Slit1 acts positively on chicken retinal axons inside the retina. First, we have shown that the retinal axons 'prefer' the area with normal amount of Slit1 to the area with low Slit1 that results from overexpression of Irx4. By rescue experiment, we have shown that Slit1 can correct the axonal phenotype that results from Irx4 overexpression, suggesting that the axonal phenotype is due to decreased *Slit1* expression. Second, we have shown that retinal axons preferentially travel above the cells that are expressing Slit1 by in vivo electroporation. Third, by gene-axon assay, we have shown that retinal axons project towards the cells that are expressing *Slit1* endogenously and that axons align with the *Slit1*-expressing cells. These results support the idea that Slit1 functions as a positive factor to the retinal axons within the retina.

Because of the complex situation in vivo, we chose to use the word 'positive' instead of 'attractive'. In vivo, several axon guidance cues co-exist in 3D space. The direction of the axonal projection may be a response to the sum of all the guidance cues present in the environment. Although the distinction is often blurred, 'positive' may be more a description of the

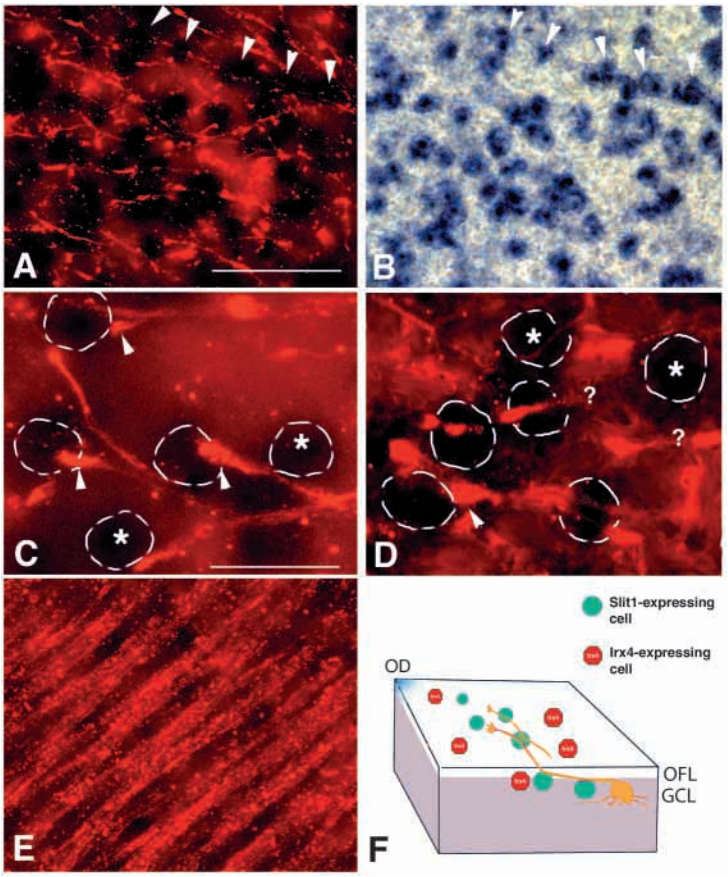

Fig. 8. Slit1 defines the trajectory of the early retinal axons in OFL. In situ hybridization was carried out on E7 retinas with the *Slit1* probe, followed by immunofluorescent staining of axons. The cells positive for the *Slit1* probe appear purple in the bright-field image (B) but appear as dark spots in the fluorescent images (A,C,D,E). Note the growth cones of the elongating axons appear to project straight towards the *Slit1*-expressing cells (arrowheads in C,D), and the early retinal axon trajectories superimposed on the *Slit1*-positive cells (arrowheads in A,B). In addition, *Slit1*-expressing cells did not appear to have axons (marked with an asterisk in C,D), and axons are likely to be extended from the cells that are negative for *Slit1* expression (marked with '?' in D). (E) Close to the optic disc, more mature axons do not align accurately with the *Slit1*-expressing cells. (F) Working model of the role of Slit1 and Irx4 in intra-retinal axon targeting.

axonal response than of the internal property of the axon guidance cues. 'Positive' also includes both 'permissive' and 'attractive' (Dodd and Jessell, 1988; Goodman, 1996). Under the current assay systems, we cannot distinguish whether the actions of Slit1 are 'permissive' or 'attractive'.

Slit1 has previously been shown to act negatively on the retinal axons by gel culture assay (Plump et al., 2002). In addition, Slit1 has also been shown to act positively to increase dendritic growth and branching of the cortical cells (Whitford et al., 2002). Several factors may account for the differences among these results. One possibility is that different extracellular matrix proteins may be present in different assays or different biological systems. The composition of the extracellular matrix is not completely clear in the OFL of the retina. It is possible that these ECM factors may modify the function of Slit1. Extracellular matrix proteins such as laminin have been shown to modulate the function of axon guidance cues including netrin 1 and Slit2 (Hopker et al., 1999; Nguyen-Ba-Charvet et al., 2001). In addition, the function of Slit1 may also be modulated by proteolytic cleavage. Slit2 is proteolytically cleaved into N-terminal and C-terminal fragments (Brose et al., 1999). In cultured DRG neurons, the N-terminal fragment (140 kDa) of Slit2 was found to promote axon branching and elongation, whereas the full-length Slit2 was inactive and may actually inhibit the activity of Slit2-N (Wang et al., 1999). Like Slit2, Slit1 is also post-translationally cleaved (Brose et al., 1999; Whitford et al., 2002; Yuan et al., 1999), although the effect of proteolytic cleavage on Slit1 function has not been reported. Interestingly, there is evidence that the Slit proteins may be processed differently in different cells (Brose et al., 1999; Whitford et al., 2002). Hence, this can be another factor contributing to the different effect of Slit1 to the axons under different assay conditions.

Our results also suggest that Slit1 mediates the retinal axon pathfinding in OFL and contributes to the generation of the 'honey comb' appearance of the early retinal axons. Slit1 does not appear to direct central projection of the retinal axons towards the optic disc. We did not detect obvious center-to-periphery gradient of *Slit1* expression. In addition, in the area that has low *Slit1* expression, the overall direction of axon projection towards the optic disc was not affected. Slit1 appears to provide short-range attraction to mediate the navigation of retinal axons across the retina in the optic fiber layer. This may be similar to what has been described as the intermediate target or 'stepping stone' phenomenon (Metin and Godement, 1996). The biological significance of the 'honey comb' appearance of the early retinal axons is currently unknown. It is possible that the scattered, non-continuous expression of *Slit1* is important to keep the attraction at a moderate level. If *Slit1* is expressed in all the cells in GCL, instead of a subset of cells, the attraction may be too strong to allow the central projection of the retinal axons.

Using electron microscopy, it has been shown that the growth cones of elongating retinal axons are positioned immediately adjacent to the neuroepithelial endfeet (Halfter and Deiss, 1984). By in situ hybridization, we analyzed *Slit1* expression during the period of active axon outgrowth, including E4.5, E6 and E9 (Fig. 2 and data not shown). At all stages analyzed, *Slit1* is consistently expressed in the ganglion cell layer (GCL), not in the inner nuclear layer (INL), where the cell bodies of the neuroepithelial or Müller glial cells reside. Therefore, *Slit1* does not appear to be expressed in neuroepithelial or Müller glial cells, but in displaced amacrine cells, based on the results of the gene-axon assay. Whether displaced amacrine cells also have 'endfeet-like' structures that might be observed in the electron microscopy with the growth cones is unclear. In addition, we also found that retinal axons at later stages did not align accurately with the *Slit1*-expressing cells. It is possible that at later stages, axon bundles are positioned immediately adjacent to neuroepithelial endfeet instead of the *Slit1*-expressing amacrine cells.

Interestingly, our results also suggest that the retinal axons seem to avoid areas in the retina with low Slit1 expression. Determining whether Slit2 provides the source for repulsion in these areas in the GCL, as *Slit2* expression is not affected by Irx4 overexpression, requires further study. It is possible that a balance between attractive and repulsive forces is required to ensure that the retinal axons travel through the optic fiber layer at the precise depth, without diving into the deeper layers of the retina or fraying towards the lens.

We thank Virginia Lee, Lin Gan, Marc Ballivet and Amy Chen for antibodies and probes; and Cliff Tabin and Neal Silverman for critical reading of the manuscript. C. L. C. is an Investigator of the Howard Hughes Medical Institute. This work was supported in part by a fellowship to Z.-Z. B. from the American Association of University Women, a grant from Charles H. Hood Foundation and a start-up fund from UMMS.

REFERENCES

Austin, C. P., Feldman, D. E., Ida, J. A., Jr and Cepko, C. L. (1995). Vertebrate retinal ganglion cells are selected from competent progenitors by the action of Notch. *Development Suppl.* **121**, 3637-3650.

Badiani, P., Corbella, P., Kioussis, D., Marvel, J. and Weston, K. (1994). Dominant interfering alleles define a role for c-Myb in T-cell development. *Genes Dev.* **8**, 770-782.

Bao, Z. Z., Bruneau, B. G., Seidman, J. G., Seidman, C. E. and Cepko, C. L. (1999). Regulation of chamber-specific gene expression in the developing heart by Irx4. *Science* **283**, 1161-1164.

Birgbauer, E., Cowan, C. A., Sretavan, D. W. and Henkemeyer, M. (2000). Kinase independent function of EphB receptors in retinal axon pathfinding to the optic disc from dorsal but not ventral retina. *Development Suppl.* **127**, 1231-1241.

Bosse, A., Zulch, A., Becker, M. B., Torres, M., Gomez-Skarmeta, J. L., Modolell, J. and Gruss, P. (1997). Identification of the vertebrate Iroquois homeobox gene family with overlapping expression during early development of the nervous system. *Mech. Dev.* **69**, 169-181.

Bosse, A., Stoykova, A., Nieselt-Struwe, K., Chowdhury, K., Copeland, N. G., Jenkins, N. A. and Gruss, P. (2000). Identification of a novel mouse Iroquois homeobox gene, Irx5, and chromosomal localisation of all members of the mouse Iroquois gene family. *Dev. Dyn.* **218**, 160-174.

Brittis, P. A., Canning, D. R. and Silver, J. (1992). Chondroitin sulfate as a regulator of neuronal patterning in the retina. *Science* **255**, 733-736.

Brittis, P. A., Lemmon, V., Rutishauser, U. and Silver, J. (1995). Unique changes of ganglion cell growth cone behavior following cell adhesion molecule perturbations: a time-lapse study of the living retina. *Mol. Cell. Neurosci.* **6**, 433-449.

Brose, K., Bland, K. S., Wang, K. H., Arnott, D., Henzel, W., Goodman, C. S., Tessier-Lavigne, M. and Kidd, T. (1999). Slit proteins bind Robo receptors and have an evolutionarily conserved role in repulsive axon guidance. *Cell* **96**, 795-806.

Brose, K. and Tessier-Lavigne, M. (2000). Slit proteins: key regulators of axon guidance, axonal branching, and cell migration. *Curr. Opin. Neurobiol.* **10**, 95-102.

Bruneau, B. G., Bao, Z. Z., Tanaka, M., Schott, J. J., Izumo, S., Cepko, C. L., Seidman, J. G. and Seidman, C. E. (2000). Cardiac expression of the ventricle-specific homeobox gene Irx4 is modulated by Nkx2-5 and dHand. *Dev. Biol.* **217**, 266-277.

Cavodeassi, F., Modolell, J. and Gomez-Skarmeta, J. L. (2001). The Iroquois family of genes: from body building to neural patterning. *Development Suppl.* **128**, 2847-2855.

Christoffels, V. M., Keijser, A. G., Houweling, A. C., Clout, D. E. and Moorman, A. F. (2000). Patterning the embryonic heart: identification of five mouse Iroquois homeobox genes in the developing heart. *Dev. Biol.* **224**, 263-274.

Cohen, D. R., Cheng, C. W., Cheng, S. H. and Hui, C. C. (2000). Expression of two novel mouse Iroquois homeobox genes during neurogenesis. *Mech. Dev.* **91**, 317-321.

Crowner, D., Madden, K., Goeke, S. and Giniger, E. (2002). Lola regulates midline crossing of CNS axons in Drosophila. *Development Suppl.* **129**, 1317-1325.

Deiner, M. S., Kennedy, T. E., Fazeli, A., Serafini, T., Tessier-Lavigne, M. and Sretavan, D. W. (1997). Netrin-1 and DCC mediate axon guidance locally at the optic disc: loss of function leads to optic nerve hypoplasia. *Neuron* **19**, 575-589.

Dodd, J. and Jessell, T. M. (1988). Axon guidance and the patterning of neuronal projections in vertebrates. *Science* **242**, 692-699.

Erskine, L., Williams, S. E., Brose, K., Kidd, T., Rachel, R. A., Goodman, C. S., Tessier-Lavigne, M. and Mason, C. A. (2000). Retinal ganglion cell axon guidance in the mouse optic chiasm: expression and function of robos and slits. *J. Neurosci.* **20**, 4975-4982.

Gomez-Skarmeta, J. L., del Corral, R. D., de la Calle-Mustienes, E., Ferre-Marco, D. and Modolell, J. (1996). Araucan and caupolican, two members of the novel iroquois complex, encode homeoproteins that control proneural and vein-forming genes. *Cell* **85**, 95-105.

Goodman, C. (1996). Mechanisms and molecules that conrol growth cone guidance. *Annu. Rev. Neurosci.* **19**, 341-377.

Halfter, W. (1985). The formation of the axonal pattern in the embryonic avian retina. *J. Comp. Neurol.* **232**, 466-480.

Halfter, W. and Deiss, S. (1984). Axon growth in embryonic chick and quail retinal whole mounts in vitro. *Dev. Biol.* **102**, 344-355.

Hamburger, V. and Hamilton, H. L. (1992). A series of normal stages in the development of the chick embryo. 1951. *Dev. Dyn.* **195**, 231-272.

Hernandez, M. C., Erkman, L., Matter-Sadzinski, L., Roztocil, T., Ballivet, M. and Matter, J. M. (1995). Characterization of the nicotinic acetylcholine receptor beta 3 gene. Its regulation within the avian nervous system is effected by a promoter 143 base pairs in length. *J. Biol. Chem.* **270**, 3224-3233.

Holmes, G. P., Negus, K., Burridge, L., Raman, S., Algar, E., Yamada, T. and Little, M. H. (1998). Distinct but overlapping expression patterns of two vertebrate slit homologs implies functional roles in CNS development and organogenesis. *Mech. Dev.* **79**, 57-72.

Hong, K., Hinck, L., Nishiyama, M., Poo, M., Tessier-Lavigne, M. and Stein, E. (1999). A ligand-gated association between cytoplasmic domains of UNC5 and DCC family receptors converts netrin-induced growth cone attraction to repulsion. *Cell* **97**, 927-941.

Hopker, V. H., Shewan, D., Tessier-Lavigne, M., Poo, M. and Holt, C. (1999). Growth-cone attraction to netrin-1 is converted to repulsion by laminin-1. *Nature* **401**, 69-73.

Hu, H. (1999). Chemorepulsion of neuronal migration by Slit2 in the developing mammalian forebrain. *Neuron* **23**, 703-711.

Hutson, L. D. and Chien, C. B. (2002). Pathfinding and error correction by retinal axons: the role of astray/robo2. *Neuron* **33**, 205-217.

Itoh, A., Miyabayashi, T., Ohno, M. and Sakano, S. (1998). Cloning and expressions of three mammalian homologues of Drosophila slit suggest possible roles for Slit in the formation and maintenance of the nervous system. *Mol. Brain Res.* **62**, 175-186.

Kidd, T., Bland, K. S. and Goodman, C. S. (1999). Slit is the midline repellent for the robo receptor in Drosophila. *Cell* **96**, 785-794.

Kramer, S. G. (2001). Switching repulsion to attraction: changing responses to slit during transition in mesoderm migration. *Science* **292**, 737-740.

Ledig, M. M., Haj, F., Bixby, J. L., Stoker, A. W. and Mueller, B. K. (1999). The receptor tyrosine phosphatase CRYPalpha promotes intraretinal axon growth. *J. Cell Biol.* **147**, 375-388.

Li, H. S., Chen, J. H., Wu, W., Fagaly, T., Zhou, L., Yuan, W., Dupuis, S., Jiang, Z. H., Nash, W., Gick, C. et al. (1999). Vertebrate slit, a secreted ligand for the transmembrane protein roundabout, is a repellent for olfactory bulb axons. *Cell* **96**, 807-818.

Liu, W., Khare, S. L., Liang, X., Peters, M. A., Liu, X., Cepko, C. L. and Xiang, M. (2000). All Brn3 genes can promote retinal ganglion cell differentiation in the chick. *Development Suppl.* **127**, 3237-3247.

Ma, Y., Certel, K., Gao, Y., Niemitz, E., Mosher, J., Mukherjee, A., Mutsuddi, M., Huseinovic, N., Crews, S. T., Johnson, W. A. et al. (2000). Functional interactions between Drosophila bHLH/PAS, Sox, and POU transcription factors regulate CNS midline expression of the slit gene. *J. Neurosci.* **20**, 4596-4605.

McLoon, S. C. and Barnes, R. B. (1989). Early differentiation of retinal ganglion cells: an axonal protein expressed by premigratory and migrating retinal ganglion cells. *J. Neurosci.* **9**, 1424-1432.

McNeill, H., Yang, C. H., Brodsky, M., Ungos, J. and Simon, M. A. (1997). mirror encodes a novel PBX-class homeoprotein that functions in the definition of the dorsal-ventral border in the Drosophila eye. *Genes Dev.* **11**, 1073-1082.

Metin, C. and Godement, P. (1996). The ganglionic eminence may be an intermediate target for corticofugal and thalamocortical axons. *J. Neurosci.* **16**, 3219-3235.

Mueller, B. K. (1999). Growth cone guidance: first steps towards a deeper understanding. *Annu. Rev. Neurosci.* **22**, 351-388.

Mummenhoff, J., Houweling, A. C., Peters, T., Christoffels, V. M. and Ruther, U. (2001). Expression of Irx6 during mouse morphogenesis. *Mech. Dev.* **103**, 193-195.

Nakamoto, M. (1996). Topographically specific effects of ELF-1 on retinal axon guidance in vitro and retinal axon mapping in vivo. *Cell* **86**, 755-766.

Nguyen Ba-Charvet, K. T., Brose, K., Marillat, V., Kidd, T., Goodman, C. S., Tessier-Lavigne, M., Sotelo, C. and Chedotal, A. (1999). Slit2-Mediated chemorepulsion and collapse of developing forebrain axons. *Neuron* **22**, 463-473.

Nguyen-Ba-Charvet, K. T., Brose, K., Marillat, V., Sotelo, C., Tessier-Lavigne, M. and Chedotal, A. (2001). Sensory axon response to substrate-bound Slit2 is modulated by lamiin and cyclic GMP. *Mol. Cell. Neurosci.* **17**, 1048-1058.

Niclou, S. P., Jia, L. and Raper, J. A. (2000). Slit2 is a repellent for retinal ganglion cell axons. *J. Neurosci.* **20**, 4962-4974.

Peters, T., Dildrop, R., Ausmeier, K. and Ruther, U. (2000). Organization of mouse Iroquois homeobox genes in two clusters suggests a conserved regulation and function in vertebrate development. *Genome Res.* **10**, 1453-1462.

Plump, A. S., Erskine, L., Sabatier, C., Brose, K., Epstein, C. J., Goodman, C. S., Mason, C. A. and Tessier-Lavigne, M. (2002). Slit1 and Slit2 cooperate to prevent premature midline crossing of retinal axons in the mouse visual system. *Neuron* **33**, 219-232.

Polleux, F., Morrow, T. and Ghosh, A. (2000). Semaphorin 3A is a chemoattractant for cortical apical dendrites. *Nature* **404**, 567-573.

Rajagopalan, S., Vivancos, V., Nicolas, E. and Dickson, B. J. (2000). Selecting a longitudinal pathway: Robo receptors specify the lateral position of axons in the Drosophila CNS. *Cell* **103**, 1033-1045.

Raper, J. A. (2000). Semaphorins and their receptors in vertebrates and invertebrates. *Curr. Opin. Neurobiol.* **10**, 88-94.

Ringstedt, T., Braisted, J. E., Brose, K., Kidd, T., Goodman, C., Tessier-Lavigne, M. and O'Leary, D. D. (2000). Slit inhibition of retinal axon growth and its role in retinal axon pathfinding and innervation patterns in the diencephalon. *J. Neurosci.* **20**, 4983-4991.

Schulte, D. and Cepko, C. L. (2000). Two homeobox genes define the domain of EphA3 expression in the developing chick retina. *Development Suppl.* **127**, 5033-5045.

Simpson, J. H., Bland, K. S., Fetter, R. D. and Goodman, C. S. (2000). Short-range and long-range guidance by Slit and its Robo receptors: a combinatorial code of Robo receptors controls lateral position. *Cell* **103**, 1019-1032.

Snow, D. M., Watanabe, M., Letourneau, P. C. and Silver, J. (1991). A chondroitin sulfate proteoglycan may influence the direction of retinal ganglion cell outgrowth. *Development Suppl.* **113**, 1473-1485.

Song, H. and Poo, M. M. (2001). The cell biology of neuronal navigation. *Nat. Cell Biol.* **3**, E81-E88.

Song, H. J. and Poo, M. M. (1999). Signal transduction underlying growth cone guidance by diffusible factors. *Curr. Opin. Neurobiol.* **9**, 355-363.

Tessier-Lavigne, M. and Goodman, C. S. (1996). The molecular biology of axon guidance. *Science* **274**, 1123-1133.

Thanos, S. and Mey, J. (2001). Development of the visual system of the chick. II. Mechanisms of axonal guidance. *Brain Res. Rev.* **35**, 205-245.

Wang, K. H., Brose, K., Arnott, D., Kidd, T., Goodman, C. S., Henzel, W. and Tessier-Lavigne, M. (1999). Biochemical purification of a mammalian slit protein as a positive regulator of sensory axon elongation and branching. *Cell* **96**, 771-784.

Whitford, K. L., Marillat, V., Stein, E., Goodman, C. S., Tessier-Lavigne,

M., Chedotal, A. and Ghosh, A. (2002). Regulation of cortical dendrite development by Slit-Robo interactions. *Neuron* **33**, 47-61.

Wu, W., Wong, K., Chen, J., Jiang, Z., Dupuis, S., Wu, J. Y. and Rao, Y. (1999). Directional guidance of neuronal migration in the olfactory system by the protein Slit. *Nature* **400**, 331-336.

Yu, T. W. and Bargmann, C. I. (2001). Dynamic regulation of axon guidance. *Nat. Neurosci. Suppl.* **4**, 1169-1176.

Yuan, W., Zhou, L., Chen, J. H., Wu, J. Y., Rao, Y. and Ornitz, D. M. (1999). The mouse SLIT family: secreted ligands for ROBO expressed in patterns that suggest a role in morphogenesis and axon guidance. *Dev. Biol.* **212**, 290-306.

Zhu, Y., Li, H., Zhou, L., Wu, J. Y. and Rao, Y. (1999). Cellular and molecular guidance of GABAergic neuronal migration from an extracortical origin to the neocortex. *Neuron* **23**, 473-485.